Chapter 2

Raman Spectroscopic Characterization of Wood and Pulp Fibers

Umesh Prasad Agarwal

Abstract

This chapter reviews applications of Raman spectroscopy in the field of wood and pulp fibers. Most of the literature examined was published between 1998 and 2006. In addition to introduction, this chapter contains sections on wood and components, mechanical pulp, chemical pulp, modified/treated wood, cellulose I crystallinity of wood fibers, and the "self-absorption" phenomenon in near-infrared (IR) Fourier-transform (FT)-Raman spectroscopy. When needed, the sections are further categorized into various subsections. For example, the section on wood and components contains a variety of topics ranging from Raman band assignments to molecular changes during tensile deformation. From this review it will become clear that Raman spectroscopy has become an essential analytical technique in the field of wood and pulp fibers.

2.1 Introduction

Techniques that can provide information on the chemical constitution of wood and pulp fibers and on processing-related changes of these materials are of great interest. Raman spectroscopy [1] is one such technique that provides fundamental knowledge on a molecular level and does not require chemical treatment of the sample (contrary to the case, for example, in fluorescence and electron microscopy). It has become an important analytical technique for nondestructive, qualitative, and quantitative analysis of materials. The technique is useful in a number of areas, including analytical measurements, mechanistic studies, and structural determinations. Studying a sample is very simple and usually involves sampling an area of interest by directing a laser excitation beam and analyzing the collected molecularly specific scattered light [2]. Although initially, obtaining good-quality Raman data required operator skill and training, this has started to change as a result of the commercial availability of compact, easy-to-use, integrated instruments at reasonable cost.

Nevertheless, although the specificity of Raman spectroscopy is very high, its sensitivity is somewhat poor. Considering that only a small number of the incident laser photons are inelastically scattered, the detection of analytes present in very low concentrations is limited. To overcome this problem, special Raman signal-enhancing techniques can be applied. The two most prominent approaches are the resonance Raman effect [3] and the

surface-enhanced Raman scattering (SERS) [4,5]. Resonance Raman and SERS are only two of many special techniques in the field of Raman spectroscopy. Nonetheless, these two techniques open the possibility of investigating low-concentration samples. Moreover, resonance Raman and SERS spectra provide additional important information about the investigated system.

In resonance Raman spectroscopy, the resonance state arises when the wavelength used to excite the Raman effect lies within the electronic absorption band of the sample, causing the vibrational modes involved in the electronic transition to be selectively enhanced (by a factor of up to 10^6 compared with nonresonant excitation). In addition, resonance Raman spectroscopy allows the site-specific investigation of chromophores within a molecule.

In Raman literature a large number of examples can be found where SERS has been used to enhance the Raman scattering of an analyte. SERS is an effect wherein a significant increase in the intensity of Raman light scattering can be observed when molecules are brought into close proximity of certain metal surfaces (e.g., Ag and Au). The metal surface should contain roughness with sizes in the order of 1/10th of the wavelength of the excitation light to obtain the largest enhancement factors. The SERS effect entails enhancement (up to 10^{11}–10^{14} times) of the Raman scattering of a molecule located in the vicinity of nanosized metallic structures (usually Ag and Au). Electromagnetic and chemical enhancement mechanisms are responsible for this effect. SERS is important not only for Raman spectroscopy but also for surface science and nanoscience. Thus, SERS-active metal surfaces serve as model substrates to investigate the type of interactions between a molecule and a substrate, the molecule's adsorption site, and, at times, the properties of such adsorbed molecules.

In studies of wood and pulp fibers, Raman spectroscopy has become an important analytical technique because of the important technical developments [6] with respect to both new instrumentation (especially instruments that successfully limit sample fluorescence) and new interpretive advances that have taken place within the past two decades. Such progress has made the macro- and microlevel Raman investigations of wood and fibers much more valuable. For instance, in the area of microinvestigations, chemical imaging of fiber cell walls has become a reality and images of cellulose and lignin distributions in the plant cell wall have provided useful information on the compositional and organizational characteristics of woody tissues [7–9].

Raman spectroscopy and its various techniques have started to have an impact on the field of wood and pulp fiber science. This chapter presents a brief overview of the recent advances. The intent of the author is to present an overview that summarizes the various capabilities of Raman spectroscopy in the field of lignocellulosics research. The chapter focuses on the characterization work published between 1998 and 2006. An earlier review by the author on the applications of Raman spectroscopy to the field of lignocellulosic materials was published in 1999 [10].

2.2 Wood and components

2.2.1 Woods

Raman spectroscopy has been applied to study both softwoods and hardwoods in their native states. Earlier studies [11–15] consisted of distinguishing these classes of woods based on chemical composition-related Raman spectral differences. Although the chemical

composition of wood is complex and varies from species to species, there are three structural polymeric components, namely, cellulose, lignin, and hemicellulose, which are common to all woods. Early on, wood spectra were assigned to various wood polymeric components [16–18]. For example, for black spruce, it was reported that observed spectral features were mostly due to cellulose and lignin [18]. Additionally, it was reported that, although present in significant quantity (20–30%), very few hemicellulose Raman contributions were detected. In more recent work [19], ultraviolet resonance Raman (UVRR) in conjunction with principal component analysis has been used to characterize woods, and using this approach, it was possible to distinguish between various aromatic and other unsaturated structures in wood.

FT-Raman spectroscopy was applied to *Eucalyptus* wood meal samples [20–28] to not only determine cell types, cell morphology, and wood constituents (α-cellulose, hemicellulose and hemicellulose sugar composition, lignin and lignin syringyl-to-guaiacyl ratio, extractives, etc.) but also to develop a rapid quantitative method for accessing wood properties for kraft pulp production. Multivariate data analysis, including cross-validation, produced highly significant correlations between conventionally measured and Raman-predicted values for a number of traits.

Nondestructive monitoring of wood decay [29] and evaluation of acid–base properties of wood [30] are two others areas of research that have taken advantage of the capabilities of FT-Raman spectroscopy. In the former case, both the C═O and the glycosidic-bond bands were used to monitor wood decay by *Coriolus versicolor*, *Dichomitus squalens*, and *Ceriporiopsis subvermispora* [29]. Next, FT-Raman spectroscopy was used to investigate the acid–base properties of bulk pine wood [30], and it was concluded that the pine was largely acidic. In the investigation, various solvents were used as probe liquids, and spectral changes at ∼2936 and ∼1657 cm^{-1} were used as measures of acid–base properties.

2.2.2 Extraneous compounds

In woods where extraneous compounds (other plant metabolites) including heartwood-resins (e.g., flavonoids and pinosylvins) were present, they have been detected using near-IR FT-Raman [31–33] and UVRR [34,35] spectroscopy. Specific bands in the spectra can be used in both wood identification and quantitative determination of specific resin compounds. For example, FT-Raman spectroscopy was used to characterize brazilwood [32] to isolate key Raman biomarker bands that could provide the basis for an identification protocol.

2.2.3 Wood components

Raman spectra of wood components – cellulose, hemicellulose, and lignin – have been obtained [18,36,37]. It is reported that lignin spectrum varies depending upon the excitation wavelength of the laser [37,38]; no such sensitivity to excitation wavelength exists in the case of cellulose and hemicelluloses. For the former, this is explicable due to the occurrence of the resonance Raman effect at shorter excitation wavelengths (UV), where different structures of lignin (*p*-hydroxyphenyl, guaiacyl, and syringyl) absorb the UV light differently. Additionally, as previously reported [39], when excited in the visible range, band intensity differences for specific modes in the spectrum of lignin arise due to pre-resonance [39] and

conjugation effects [40]. Of the Raman spectra of three polymer components, only cellulose spectrum has been well characterized and assigned [36,41], although high degree of coupling exists between vibrations that involve C—C and C—O bonds. This knowledge has helped in the interpretation of wood and pulp fiber spectra. Considering that the Raman spectra of lignins (syringyl, guaiacyl, and coumaryl) are complex, significant advances have been made to interpret them. This has come about as a result of studying, with a number of approaches, not only lignins (native [18], milled wood [18,42,43], and residual lignins [37,44–47]) and their models (deuterated and normal dehydrogenation polymer [DHP] lignins [48] and a large number of lignin model compounds [38,49]) but also chemically modified (e.g., bleaching, hydrogenation, and acetylation) lignins and lignocellulosics [10,39,43,50,51]. An additional tool in the aid to interpretation has been the theoretical calculations on lignin models wherein some degree of preliminary work has been done [52,53], but a lot more remains. In recently reported research findings, an additional approach, partial least squares modeling, was successfully used to interpret the UVRR spectra of lignin model compounds [54].

Considering that lignin's heterogeneous structure consists not only of interphenylpropane-unit linkages of carbon-to-carbon and carbon-to-oxygen but also of side chains with various substituent and functional groups, a study of a large number of representative models is essential. In the work recently completed in the author's laboratory [49], 40 lignin models were investigated (Figure 2.1) in the neat state (near-IR FT-Raman and FT-IR), in solution (near-IR FT-Raman), and on cellulose (near-IR FT-Raman). These models represent a large number of substituent/functional groups and substructures in lignin–aliphatic and phenolic OH, C═O, CHO, COOH, CH_3, OCH_3, α,βC═C, furan, and interunit C—O—C and C—C linkages. Raman band positions associated with various groups were identified and Raman frequencies and intensities were compared between the models. The position of the 1600 cm^{-1}-Raman-mode was found to be only minimally sensitive to substituents because in ~70% of the models, including those containing more than one phenyl group, the vibrational frequency was confined between 1594 and 1603 cm^{-1}. Sensitivity of a model's vibrational frequencies to its environment was evaluated by comparing frequency data in three different sampling states – in neat, in solution, and on cellulose. Several Raman band positions shifted compared to the value in the neat state.

2.2.4 Band assignments

The Raman spectra of wood and pulp fibers were assigned to the three polymer components and, in the case of lignin, further to its substructural units. Such interpretation of the experimental Raman data was based on pure-component spectra and their assignments. However, sometimes, a clear assignment of the measured Raman band to specific vibration is unclear. To further improve this situation, an assignment of the observed Raman bands can be assisted by a systematic comparison with the theoretically calculated spectra [52,53]. Although quantum chemical calculations and normal coordinate analysis have been available for sometime, recently it was shown that density functional theory (DFT) methods provide a powerful alternative, as they are much less computationally demanding (compared with the quantum calculations) and take account of the effects of electron correlation. Recently, a DFT method using the B3LYP functional and 6-31 + G(d) basis set was used to

	R_1	R_2	R_3	R_4
1	–COOH	–H	$–OCH_3$	–H
2	–COOH	$–OCH_3$	$–OCH_3$	–H
3	–CH=CHCHO	–H	$–OCH_3$	–H
4	–H	$–OCH_3$	–OH	$–OCH_3$
5	O $–CCH_3$	$–OCH_3$	$–OCH_3$	–H
6	O $–CCH_3$	$–OCH_3$	–OH	–H
7	figure	–H	–H	–H
8	–CH=CHCOOH	–H	$–OCH_3$	–H
9	–H	$–OCH_3$	$–OCH_3$	–H
10	O $–CCH_3$	$–OCH_3$	O –OCCH3	–H
11	O $–CCH_3$	–H	–H	–H
12	–CHO	$–OCH_3$	$–OCH_3$	–H
13	O $–CCH_3$	–H	–OH	–H
14	–CH=CHCOOH	$–OCH_3$	–OH	–H
15	O $–CCH_3$	$–OCH_3$	$–OCH_3$	$–OCH_3$
16	figure	$–OCH_3$	–OH	–H
17	–CH=CHCOOH	$–OCH_3$	–OH	$–OCH_3$
18	$–CH_2OH$	–H	–OH	–H
19	figure	–H	figure	–H
20	O $–CCH_3$	–H	figure	–H

	R_1	R_2	R_3	R_4
21	O $–CCH_2CH_3$	$–OCH_3$	–OH	$–OCH_3$
22	figure	$–OCH_3$	$–OCH_3$	–H
23	figure	$–OCH_3$	–OH	–H
24	figure	$–OCH_3$	$–OCH_3$	–H
25	OH $–CHCH_3$	$–OCH_3$	$–OCH_3$	–H
26	$–CH_3$	$–OCH_3$	–OH	–H
27	$–CH_2OH$	$–OCH_3$	$–OCH_3$	–H
28	$–CH_3$	$–OCH_3$	O $–OCCH_3$	–H
29	$–CH_2OH$	–H	$–OCH_3$	–H
30	$–CH_2CH_2CH_3$	$–OCH_3$	–OH	–H
31	$–CH=CHCH_3$	$–OCH_3$	–OH	–H
32	–COOH	$–OCH_3$	–OH	–H
33	–CHO	–OH	$–OCH_3$	–H
34	–CHO	$–OCH_3$	–OH	–H
35	–COOH	$–OCH_3$	–OH	$–OCH_3$
36	–CHO	$–OCH_3$	–OH	$–OCH_3$
37	–CH=CHCOOH	–H	–OH	–H
38	–COOH	–H	–OH	–H
39	–CHO	$–OCH_3$	$–OCH_3$	$–OCH_3$
40	O $–CCH_3$	$–OCH_3$	–OH	$–OCH_3$

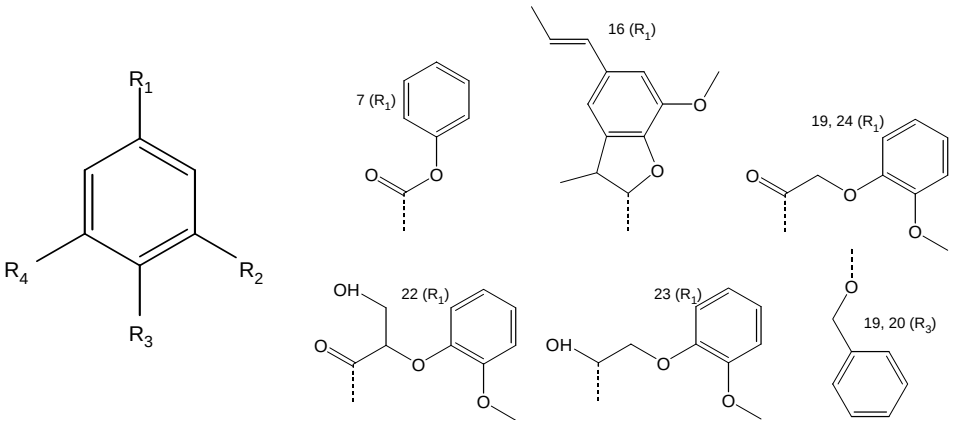

Figure 2.1 Molecular structures of 40 lignin models used in the lignin model study.

predict the vibrational frequencies of some simple lignin models [53]. The performance of this DFT method was evaluated by comparison of the computed frequencies with observed Raman spectra of the appropriate model compounds. Assignments for vibrational bands of the lignin polymer were presented. In future, this approach is expected to result in reliable assignment of those experimentally observed lignin Raman bands that have not yet been properly assigned, which in turn will lead to a detailed understanding of the geometrical and electronic structure of the investigated molecular lignin model units.

2.2.5 Microscope studies

Although Raman microscopy (lateral spatial resolution ~1.0 μm) preceded IR microscopy (resolution ~10 μm) commercially by ~5 years, infrared microscopy has been used more often in the past. Currently easier to use and increasingly available, Raman microscopy is being used more frequently. In the investigations of wood and pulp fibers, Raman studies range from investigating tensile deformation of single wood fibers [55,56] to detailed investigations, at the subcellular level, of composition and ultrastructure of native woody tissue [7–9].

Indeed, in the early years of wood investigations by Raman using the 514.5 nm argon ion laser excitation, a Raman microprobe was more successful because of its ability to circumvent the sample fluorescence, which invariably accompanied the Raman signal. Moreover, subsequently, with the availability of the 633- and 785-nm-laser-based Raman microscopy systems, the fluorescence interference has been further minimized. Consequently, it became realistic to investigate individual morphological regions in the woody tissue and spectra at high spatial resolution could be obtained. Although a resolution of 1 μm (obtained using a 100× microscope objective) in Raman spectroscopy is limited due to the diffraction effect, compared with IR microscopy, it is 10 times better. It was polarized Raman microscopy that showed, for the first time, that secondary wall lignin was ordered [16,17]. The recent technological advances [6] have benefited Raman microscopy instrumentation extensively and a state-of-the-art system is capable of providing new information at the individual cell wall morphological level [9].

2.2.6 Fiber cell wall organization and compositional heterogeneity

As mentioned earlier, with a confocal Raman microscope spectra of a very small sample-volume can be measured, and therefore, the chemical composition of very small structures can be determined. For heterogeneous samples such as wood fibers, the distributions of cellulose and lignin are important. Such information can be obtained with a Raman microscope that provides images based on a Raman band characteristic for the component of interest [18]. In cell wall Raman imaging, inherent scattering characteristics of cellulose and lignin are used to visualize their distribution and no external labels are necessary [8,9]. In confocal Raman microscopy, point-by-point imaging couples the mobility of an automated scanning stage with the high numerical aperture of the microscope objective to take the spectrum at each sample point. The technique has been used to study micron-size regions in the fiber cell wall.

Although, in the studies of wood fibers, use of Raman microscopy preceded macro-investigations, the progress towards detailed cell wall investigations was hindered due to the limitations driven by both sampling and instrumentation. Sample fluorescence and a lignin band that was less than fully stable made Raman microscopy investigations difficult. In addition, a highly efficient Raman microprobe equipped with an automated high-resolution x, y stage was not available. In the 1990s, new technologies such as the holographic notch filter and the availability of charge-coupled devices that acted as multichannel detectors decreased acquisition time by more than an order of magnitude. Rugged, air-cooled lasers (e.g., He–Ne 633 nm) simplified utility requirements and provided more beam-pointing stability compared with that of water-cooled lasers. Furthermore, sampling in confocal mode reduced fluorescence by physically blocking the signal originating from the volume of the sample not in focus. The detected Raman signal came from the illuminated spot. The latest Raman microprobe incorporates these advances and is well suited to investigate lignin and cellulose distribution in the cell walls of woody tissue. These capabilities permit compositional mapping of the woody tissue with chosen lateral and axial spatial resolutions.

Most recent applications of confocal Raman microscopy to woody cell walls consisted of chemical imaging of poplar (including the tension wood) and spruce woods [8,9] as well as topochemical studies of beech wood [7]. In the case of spruce [9], a state-of-the-art 633-nm-laser-based confocal Raman microscope was used to determine the distribution of cell wall components in the cross section of black spruce wood *in situ*. Chemical information from morphologically distinct cell wall regions was obtained and Raman images of lignin and cellulose spatial distribution were generated. While cell corner (CC) lignin concentration was the highest on average, lignin concentration in compound middle lamella (CmL) was not significantly different from that in secondary wall (S2 and S2–S3). Images generated using the 1650 cm^{-1} band showed that coniferaldehyde and coniferyl alcohol distribution followed that of lignin and no particular cell wall layer/region was therefore enriched in the ethylenic residue. In contrast, cellulose distribution showed the opposite pattern – low concentration in CC and CmL and high in S2 regions. Nevertheless, cellulose concentration varied significantly in some areas, and concentrations of both lignin and cellulose were high in other areas. Figure 2.2a, taken from Reference 9, shows the bright field image of the cell wall area that was investigated by Raman microscopy. Chemical images, indicating lignin and cellulose distributions, are shown in Figure 2.2b and c, respectively.

Besides using visible laser excitation in Raman microscopy, for the first time, use of UVRR (244 nm excitation) to study individual plant cell walls has been reported [57]. Because damage to the cell walls is expected at such high-energy wavelengths of excitation, a series of spectra were obtained along a given cell wall at low power and for short duration. These were then averaged to produce a mean spectrum with a high signal-to-noise ratio and represented that region of the cell wall.

2.2.7 Molecular changes during tensile deformation

In other studies of wood fibers [55,56], Raman microscopy was used to show that during tensile deformation the $\sim$1095 cm^{-1} Raman band shifts towards a lower wave number due to molecular deformation of cellulose. This shift has been shown to be useful in understanding the micromechanisms of deformation in wood and pulp fibers. In one study [56],

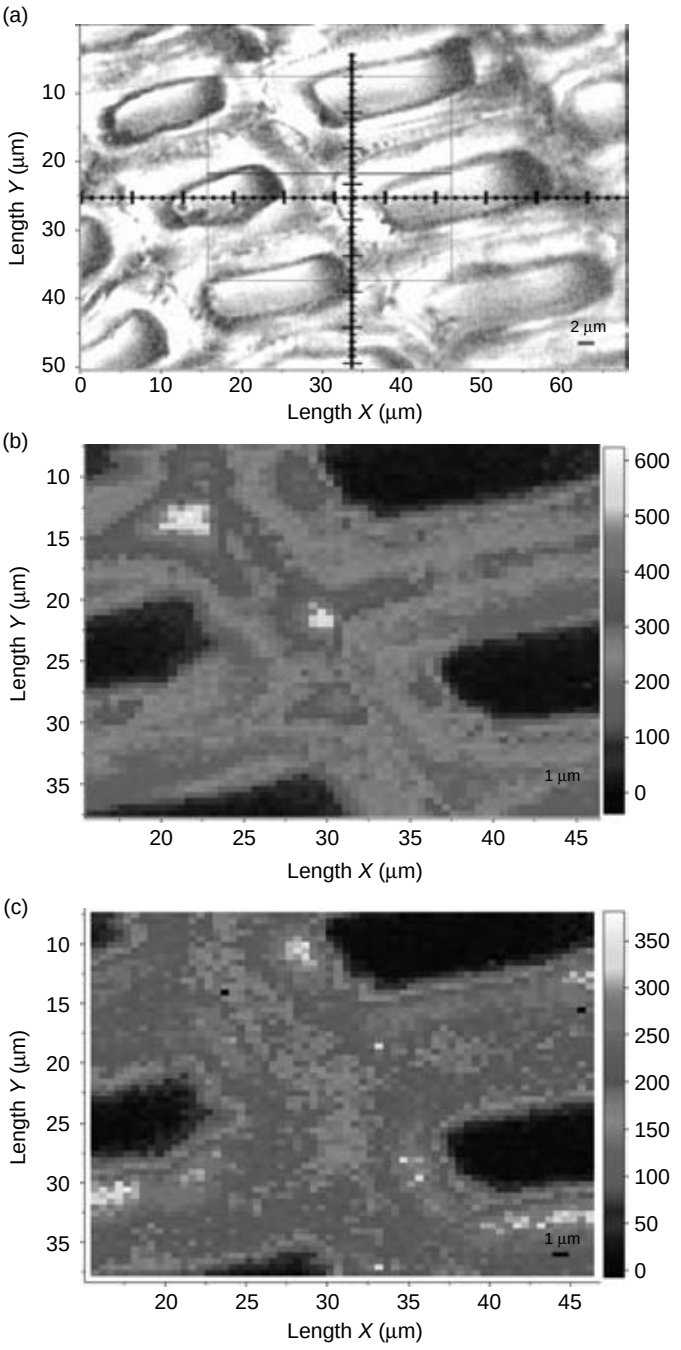

Figure 2.2 See opposite page for caption.

isolated fibers of spruce latewood were mechanically strained and molecular changes due to deformation were monitored by stress–strain curves and changes in band positions and intensities. Frequency changes for the 1097 cm^{-1} band correlated well with the applied stress and strain. Additionally, a decrease in the peak intensity ratio of the 1127 and 1097 cm^{-1} bands was related to the straining of the latewood fiber. Changes observed in the O—H stretch region were interpreted in terms of weakening of the hydrogen-bonding network as a result of straining. Stretching of the spruce fiber was found to have no influence on lignin Raman bands.

2.3 Mechanical pulp

Bleaching of spruce thermomechanical pulp by alkaline hydrogen peroxide, sodium dithionite, and sodium borohydride was studied using FT-Raman spectroscopy [50]. The Raman examination revealed that spectral differences between bleached and unbleached pulp fiber spectra were primarily due to coniferaldehyde and *p*-quinone structures in lignin. This was new direct evidence that such bleaching removes *p*-quinone structures. In the unbleached pulp, the contribution of *p*-quinones was detected in the 1665–1690 cm^{-1} region. This contribution was removed to varying degrees in the bleached pulps, depending on the extent to which the pulps were brightened. As shown in Figure 2.3, the relative change in the post-color number of the pulp correlated linearly with the Raman intensity decline in the 1665–1690 cm^{-1} region. Although the correlation was not great, it nonetheless indicated that *p*-quinone structures were largely responsible for determining pulp brightness.

FT-Raman and other spectroscopic methods were used to detect lignin oxidation products in thermomechanical pulp (TMP) [58]. It was shown that using 2,2′-azinobis-3-ethylbenzthiazoline-6-sulfonate cation radical ($ABTS^{\bullet+}$) and FT-Raman spectroscopy, detailed information on lignin reactions can be obtained. Another approach [59] in probing lignin structure by ($ABTS^{\bullet+}$) was to make use of the pre-resonance and resonance Raman techniques in conjunction with the Kerr gate. The Kerr gate approach permits temporary rejection of high level of fluorescence from resonance Raman spectra. Spectral information obtained depended upon both the wavelength of excitation and lignin excitation profiles.

Figure 2.2 (a) Bright-field image of spruce cross section (micrometer scale superimposed) showing selected area (red rectangle) for Raman mapping. Rectangle encloses cell walls of six adjoining mature tracheid cells and contains three CC regions. Raman images of this area are shown in (b) lignin and (c) cellulose. A *Y*-segment at $Y = 21.6$ μm is marked; from Reference 9. For a better visual illustration, see the colored figure in the reference. (b) Raman image (false color) of lignin spatial distribution in selected cell wall area in (a) in two-dimensional representation. Intensity scale appears on the right. Bright white/yellow locations indicate high concentration of lignin; dark blue/black regions indicate very low concentration, for example, lumen area; from Reference 9. See Plate 1 for the color image. (c) Raman images (false color) of cellulose spatial distribution in cell wall area selected in (a) in two-dimensional representation. Bright white/yellow locations indicate high cellulose concentration; dark blue/black regions indicate very low concentration, for example, lumen area; from Reference 9. See Plate 2 for the color image. (From Agarwal [9].)

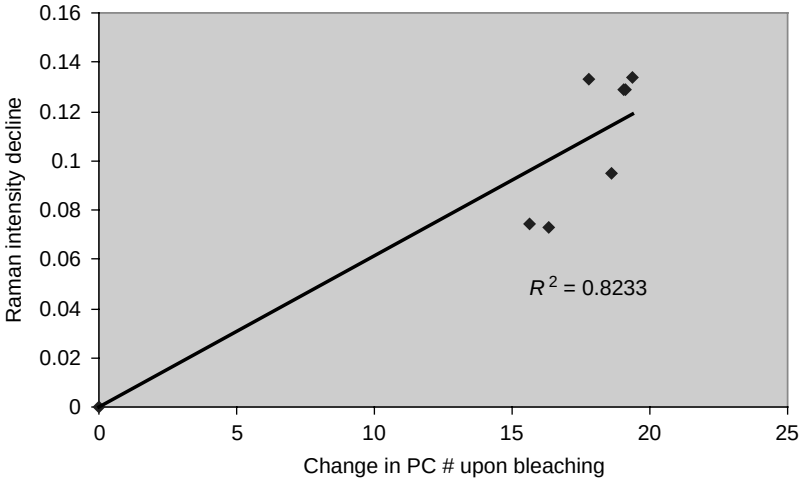

Figure 2.3 Linear regression between ΔPC and the decline in Raman intensity of the 1665–1690 cm^{-1} region (contribution primarily due to *p*-quinones).

Hydrothermally degraded ground-wood-fibers containing paper (75% ground wood and 25% bleached sulfite) was studied with the help of near-IR Raman spectroscopy [60]. Degradation reactions were monitored by observing the appearance of C═O stretching bands upon formation of carbonyl containing species. However, other changes that resulted in the C═C band intensity decline suggested involvement of the coniferyl alcohol groups.

Photochemically modified mechanical pulp fibers in printing and writing papers were investigated by both macro- and micro-FT-Raman spectroscopy to determine the extent to which aromatic lignin structure was destroyed [61]. In the microscopic study, 10 spots through the thickness of the paper were analyzed, and the ratio of aromatic to cellulose vibration intensity (I_{1600}/I_{1095}) was calculated. The results showed the destruction of aromatic structures on the photoexposed surface, as well as an increase in aromatic structure intensity deeper in the sheet. This increased intensity was attributed to C═O bonds formed on the aromatic structures during initial stages of photo-oxidation. Macro-Raman analysis revealed that upon photo-oxidation the band at 1654 cm^{-1} decayed and a new band appeared at 1675 cm^{-1}, indicating destruction of ring conjugated C═C structures and formation of *p*-quinone structures.

Bleaching and photoyellowing of TMPs was also studied using UV–vis and resonance Raman spectroscopy [62]. In the latter technique, the chosen excitation wavelength was close to the absorption bands of the light-generated chromophores to take advantage of the resonance enhancement. The results revealed that the originally present coniferaldehyde structures were partly removed by alkaline peroxide bleaching and they were further degraded upon light exposure. On the basis of the resonance Raman analysis of the photoexposed pulps, formation of quinone structures, possibly *p*-quinones, was found to be a plausible explanation for the brightness reversion of the pulps.

The cause of darkening in biomechanical pulp was investigated by FT-Raman and other spectroscopy techniques [63]. The results indicated that quinones (both *o*- and *p*-) were

produced when wood chips were treated with the fungus. This was also the case when fungus-treated wood chips were refined at higher steaming pressures (up to 85 psi). For a given pressure, compared with control pulps, treated pulps were darker because their quinone content was higher. Within the set of biopulps that were produced at various steaming pressures, higher-pressure pulps were darker and contained more quinones.

2.4 Chemical pulp

Using conventional Raman spectroscopy fully bleached chemical pulp fibers have been studied earlier in the 1980s and differences in the pulp spectra were found to exist [64]. However, due to the problem of fluorescence associated with unbleached and partly bleached pulps, these could not be investigated and their Raman studies have to wait until near-IR-excited FT-Raman technique was developed. Fluorescence signal was minimized in FT-Raman spectroscopy and the technique was well suited to investigate residual lignin in chemical pulps. Lignin in pine kraft pulps was quantified by FT-Raman based on the ratio of the lignin and cellulose band intensities [44]. The data was found to correlate well with the kappa number of the pulps. However, because in FT-Raman only a single prominent lignin band at 1600 cm^{-1} was observed in the pulp spectra, it was still not possible to obtain information on the detailed residual lignin structural changes that were being introduced by the bleaching chemicals.

UVRR spectroscopy was used [37,46,47,65] not only for determination of lignin in unbleached and fully bleached chemical pulps, but also to detect bleaching-related changes in residual lignin. Both lignin and hexenuronic acid could be investigated. Whereas concentration of lignin was predicted fairly accurately, the standard error of prediction was higher for hexenuronic acid [65]. The UVRR method was found to be highly sensitive and selective for detecting lignin structures.

In another application of resonance Raman spectroscopy to detect highly fluorescent residual lignin in chemical pulps, optical Kerr gate approach was successfully used [47]. Sample fluorescence was effectively suppressed and much weaker bands of lignin could be observed and information on chromophore groups in pulps could be obtained.

Recently, in the author's laboratory, for the first time, SERS effect in unbleached kraft pulp fibers was induced using nano- and microparticles of silver (Figure 2.4) [66]. Further, it was shown that only residual lignin bands were enhanced in intensity. The lack of carbohydrate signal enhancement implied that SERS method can be used to selectively investigate lignin in presence of carbohydrate polymers. The structural transformations of lignin in pulps bleached with polyoxometallates were investigated using SERS [45].

In addition to studies of residual lignin in pulps, a small amount of carbonyl groups in cellulose pulps (μmol/g range), have been investigated by a combination of carbonyl-selective fluorescence labeling method and UVRR. It was demonstrated [67] that carbonyls in the pulps are not only present as a C═O structure with an sp^2-hybridized carbon, but also to a significant extent in sp^3-hybridized form as hydrates or hemiacetals.

FT-Raman technique has been applied to the area of wood pulp recycling. In one study [68], the composition of recycled pulp (including pigments such as calcium carbonate, talc, gypsum, titanium dioxide and kaolin) was analyzed whereas in the other [69] structural change in cellulose was the subject of investigation.

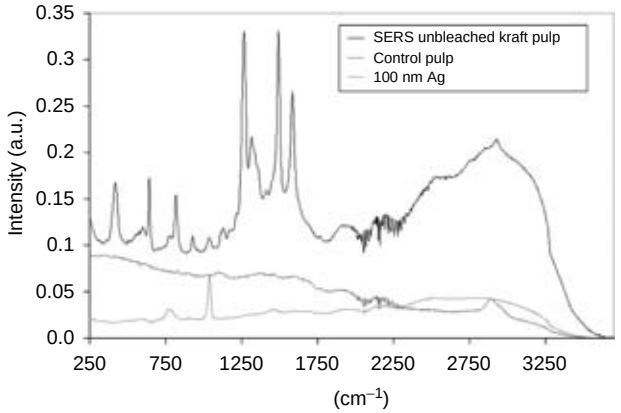

Figure 2.4 Near-IR FT-Raman spectra of various samples: top, SERS of ball-milled unbleached KP (pulp-to-Ag weight ratio 1:1); middle, normal spectrum of same pulp without Ag; bottom, spectrum of 100–150 nm Ag particles. Spectra have been vertically offset for improved visualization. In the pulp SERS spectrum, most enhanced bands were present between 250 and 1800 cm^{-1}. In normal pulp spectrum (middle) hardly any peaks were detected due to high sample fluorescence.

2.5 Modified/treated wood

2.5.1 Heat treated

Thermal modification of woods was studied by examining chemical changes in wood structure by UVRR spectroscopy [70]. It was found that upon heat treatment at 180°C or higher lignin became partly soluble in acetone. Spectra of extracted wood samples indicated that the structure of unextracted lignin remained unchanged when heated to 200°C. Additionally, formation of new carbonyl groups was reported and it was found that the lignin content of the samples was increased as a result of degradation of wood hemicelluloses.

In one study that used FT-Raman to look at the pyrolyzed Japanese cedar [71] in a nitrogen atmosphere at various temperatures (200–1000°C), observation of two characteristic bands at 1340 and 1590 cm^{-1} was reported and the spectral features were found to change markedly as a function of temperature. A second study [72] involved Raman investigations of Japanese larch heartwood and Japanese beech sapwood where the wood samples were heated for 22 h at constant temperatures in the temperature range of 50–180°C. The spectral changes, mainly detected in the C═C and C═O regions, were interpreted in terms of condensation reactions of lignin during heat treatment. At higher temperatures, spectral changes in the region 1200–1500 cm^{-1} suggested that the wood constituents were partly decomposed.

2.5.2 Chemically treated

Propiconazole, a fungistatic agent, has a Raman band in the region 647–693 cm^{-1}. Using a 785-nm-laser-excited conventional microprobe, the band intensity in the latter region was used to determine the propiconazole distribution in white spruce [73]. The Raman study

of longitudinal depth distribution pattern of propiconazole correlated well with the gas chromatography–mass spectroscopy (GC–MS) profile.

A Raman microscopic investigation to measure the melamine–formaldehyde resin content within cell walls of impregnated spruce wood was carried out [74] and the findings were compared with the UV method. Not only Raman was found to be a good method for estimating the resin content, the sharpness of the Raman melamine peak compared with the not-well-defined increase in the UV absorbance was an added advantage in the Raman analysis. Previously, FT-Raman spectroscopy was used for characterization of melamine–formaldehyde resins [75].

Additionally, identification of adhesives in wood has been carried out using FT-Raman method [76]. For example, wood adhesives such as urea resins, melamine resins, phenolic resins, resorcinol resins, and vinyl acetate resins were studied. How spectral features were affected upon curing was also evaluated, and the FT-Raman method was shown to be a useful nondestructive analytical technique to investigate synthetic resins in wood.

Because of environmental benefits, boron compounds are often used for preservative treatment of wood as they are less toxic to mammals while being regarded as both an effective insecticide and fungicide. FT-Raman spectroscopy was used to understand the role of boric acid in Japanese cedar wood [77]. A symmetrical stretching vibrational band of BO_3 group at 879 cm^{-1} was used to study boric acid distribution of two different types of wood blocks treated in aqueous boric acid solution, one cross-sectional and one longitudinal. It was concluded that from the intensity and peak position of the Raman band due to $B(OH)_3$, the $B(OH)_3$ unit in wood can be classified into two groups based on the chemical species around it. One group comprises the microcrystalline state of $B(OH)_3$ precipitated in the lumens, and the other comprises the $B(OH)_3$ units penetrating the cell wall. An obvious tendency recognized from the Raman line maps in the longitudinal direction was that $B(OH)_3$ microcrystals were made significantly more abundant near the cut ends in a longitudinal wood block due to the air-drying process.

2.6 Cellulose I crystallinity of wood fibers

Using near-IR FT-Raman spectroscopy and Whatman CC31 cellulose samples that were partially crystalline, a cellulose I crystallinity estimation model based on the Raman band intensity ratio of the 378 and 1096 cm^{-1} bands was developed [78]. This model was then used to calculate cellulose I crystallinity in sour orange (a hardwood). Raman determined crystallinity values of wood cellulose were reliable and produced low standard error. To detect if cellulose crystallinity changed in trees that were grown under elevated CO_2 climate conditions, the FT-Raman model was used. No significant change in cellulose crystallinity was found (Figure 2.5) although mean values varied between 46% and 51% and one of the control samples (SOAC#7 in Figure 2.5) showed slightly higher absolute cellulose crystallinity. While "crystallinity determination by Raman" work is ongoing, it is expected that the Raman method will be applicable to fibers of softwoods, hardwoods, and pulps.

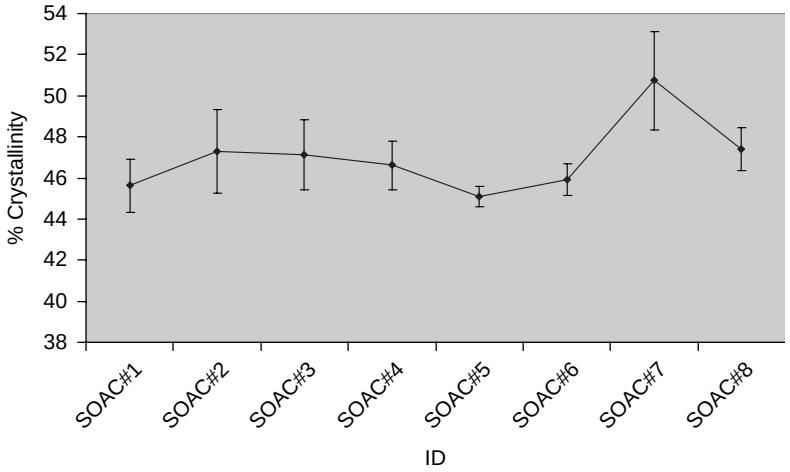

Figure 2.5 Cellulose I crystallinity of sour orange (hardwood) acid chlorite-delignified (SOAC) stem wood calculated using the FT-Raman method; Controls – #1, #2, #7 and #8, and elevated CO_2 – #3–#6; Error bars represent mean ± SD.

2.7 "Self-Absorption" phenomenon in near-IR FT-Raman spectroscopy

Cellulose and lignocellulosic materials can be conveniently studied using near-IR FT-Raman spectroscopy, and the problem of laser-induced fluorescence can be avoided or minimized. However, it was reported [79] that in the FT-Raman spectral region 2800–3500 cm^{-1} the phenomenon of self-absorption (defined as absorption of Raman scattered photons by the sample itself) occurs, and therefore, the Raman intensity of bands in this region diminishes. This was a study where Whatman cellulose paper and spruce TMP samples were studied and the self-absorption effect was found to suppress the intensity of the 2895 cm^{-1} Raman band in the C—H stretch region. Experimental observations indicated that such suppression was caused by cellulose in both the samples, and lignin, in the case of pulp, was not implicated. Furthermore, hydroxyl groups present in cellulose/hemicellulose and water were suspected to have played a role. Although certain precautions can be taken in FT-Raman quantitative work to minimize the detrimental effect of this phenomenon, it is best to choose a band in the spectrum that is not part of the C—H stretch region.

Conclusions

As a material characterization technique, Raman is complementary to IR and both must be used to obtain comprehensive information on samples. The field of Raman spectroscopy has benefited immensely from recent technological advantages in instrumentation. Because of such advances, at present, wood and pulp fiber materials can be studied using UV-, visible-, and near-IR-Raman methods. Application of Raman methods to wood and

pulp fibers covers wide and diverse research areas. In fundamental and applied research, the technique has produced useful insights and generated new information. Using the traditional approaches, not only large areas of wood and fiber samples have been investigated but, with the help of a confocal Raman microscope, sample domains as small as 1.0 μm have been analyzed and chemical images generated. This review convincingly demonstrates that Raman spectroscopy has become an indispensable analytical method for studying wood and pulp fiber materials.

References

1. Schmitt, M.; Popp, J., Raman Spectroscopy at the Beginning of the Twenty-First Century; *J. Raman Spectrosc.* 2006, 37, 20–28.
2. Ferraro, J.R.; Nakamoto, K.; Ferraro, J., *Introductory Raman Spectroscopy*, 2nd Edition; Academic Press, New York, 2003.
3. Long, D.A., *Raman Spectroscopy*; McGraw Hill, New York, 1977, Chapter 7.
4. Campion, A.; Kambhampti, P., Surface-Enhanced Raman Scattering; *Chem. Soc. Rev.* 1998, 27, 241–250.
5. Moskovits, M., Surface-Enhanced Raman Spectroscopy: A Brief Retrospective; *J. Raman Spectrosc.* 2005, 36, 485–496.
6. Adar, F., Evolution and Revolution of Raman Instrumentation – Application of Available Technologies to Spectroscopy and Microscopy. In: Lewis, I.R.; Edwards, H.G. (eds); *Handbook of Raman Spectroscopy*; Marcel Dekker Inc, New York, 2002; pp. 11–40.
7. Roder, T.; Koch, G.; Sixta, H., Application of Confocal Raman Spectroscopy for the Topochemical Distribution of Lignin and Cellulose in Plant Cell Walls of Beech Wood (*Fagus sylvatica* L.) Compared to UV Microspectrophotometry; *Holzforschung* 2004, 58, 480–482.
8. Gierlinger, N.; Schwanninger, M., Chemical Imaging of Poplar Wood Cell Walls by Confocal Raman Microscopy; *Plant Physiol.* 2006, 140, 1246–1254.
9. Agarwal, U.P., Raman Imaging to Investigate Ultrastructure and Composition of Plant Cell Walls: Distribution of Lignin and Cellulose in Black Spruce Wood (*Picea mariana*); *Planta* 2006, 224, 1141–1153.
10. Agarwal, U.P., An Overview of Raman Spectroscopy as Applied to Lignocellulosic Materials. In: Argyropoulos, D.S. (ed.); *Advances in Lignocellulosics Characterization*; TAPPI Press, Atlanta, GA, 1999; pp. 201–225.
11. Kenton, R.C.; Rubinovitz, R.L., FT-Raman Investigations of Forest Products; *Appl. Spectrosc.* 1990, 44, 1377–1380.
12. Evans, P.A., Differentiating "Hard" from "Soft" Woods Using Fourier Transform Infrared and Fourier Transform Raman Spectroscopy; *Spectrochim. Acta* 1991, 47A, 1441–1447.
13. Lewis, I.R.; Daniel, Jr., N.W.; Chaffin, N.C.; Griffiths, P.R., Raman Spectrometry and Neural Networks for the Classification of Wood Types–1; *Spectrochim. Acta* 1994, 50A, 1943–1958.
14. Yang, H.; Lewis, I.R.; Griffiths, P.R., Raman Spectrometry and Neural Networks for the Classification of Wood Types. 2. Kohonen Self-Organizing Maps; *Spectrochim. Acta Mol. Biomol. Spectrosc.* 1999, 55A, 2783–2791.
15. Lavine, B.K.; Davidson, C.E.; Moores, A.J.; Griffiths, R.P., Raman Spectroscopy and Genetic Algorithms for the Classification of Wood Types; *Appl. Spectrosc.* 2001, 55, 960–966.
16. Atalla, R.H.; Agarwal, U.P., Raman Microprobe Evidence for Lignin Orientation in the Cell Walls of Native Woody Tissue; *Science* 1985, 227, 636–638.

17. Agarwal, U.P.; Atalla, R.H., *In-situ* Raman Microprobe Studies of Plant Cell Walls: Macromolecular Organization and Compositional Variability in the Secondary Wall of *Picea mariana* (Mill.) B.S.P.; *Planta* 1986, 169, 325–332.
18. Agarwal, U.P.; Ralph, S.A., FT-Raman Spectroscopy of Wood: Identifying Contributions of Lignin and Carbohydrate Polymers in the Spectrum of Black Spruce (*Picea mariana*); *Appl. Spectrosc.* 1997, 51, 1648–1655.
19. Nuopponen, M.H.; Wikberg, H.I.; Birch, G.M. *et al.*, Characterization of 25 Tropical Hardwoods with FT-IR, Transform Infrared, Ultraviolet Resonance Raman, and 13C-NMR Cross-Polarization/Magic-Angle Spinning Spectroscopy; *J. Appl. Poly. Sci.* 2006, 102, 810–819.
20. Ona, T.; Sonoda, T.; Ito, K. *et al.*, Rapid Determination of Cell Morphology in Eucalyptus Wood by Fourier Transform Raman Spectroscopy; *Appl. Spectrosc.* 1999, 53,1078–1082.
21. Ona, T.; Sonoda, T.; Ito, K. *et al.*, *In Situ* Determination of Proportion of Cell Types in Woods by FT-Raman Spectroscopy, *Anal. Biochem.* 1999, 268, 43–48.
22. Ona, T.; Sonoda, T.; Ito, K. *et al.*, Quantitative FT-Raman Spectroscopy to Measure Wood Cell Dimensions, *Analyst* 1999, 124, 1477–1480.
23. Ona, T.; Ohshima, J.; Adachi, K.; Yokota, S.; Yoshizawa, N., Length Determination of Vessel Elements in Tree Trunks Used for Water and Nutrient Transport by Fourier Transform Raman Spectroscopy; *Anal. Bioanal. Chem.* 2004, 380, 958–963.
24. Ona, T.; Sonoda, T.; Ito, K.; Shibata, M.; Kato, T.; Ootake, Y., Non-destructive Determination of Hemicellulosic Neutral Sugar Composition in Native Wood by Fourier Transform Raman Spectroscopy; *J. Wood Chem. Technol.* 1998, 18, 43–51.
25. Ona, T.; Sonoda, T.; Ito, K. *et al.*, Non-Destructive Determination of Lignin Syringyl/Guaiacyl Monomeric Composition in Native Wood by Fourier Transform Raman Spectroscopy*; J. Wood Chem. Technol.* 1998, 18, 27–41.
26. Ona, T.; Sonoda, T.; Ito, K.; Shibata, M.; Kato, T.; Ootake, Y., Determination of Wood Basic Densities by Fourier Transform Raman Spectroscopy; *J. Wood Chem. Technol.* 1998, 18, 367–379.
27. Ona, T.; Sonoda, T.; Ito, K. *et al.*, Rapid Prediction of Pulp Properties by Fourier Transform Raman Spectroscopy of Native Wood*; J. Pulp Paper Sci.* 2000, 26, 43–47.
28. Ona, T.; Ohshima, J.; Adachi, K.; Yokota, S.; Yoshizawa, N., A Rapid Quantitative Method to Assess Eucalyptus Wood Properties for Kraft Pulp Production by FT-Raman Spectroscopy; *J. Pulp Paper Sci.* 2003, 29, 6–10.
29. Wariishi, H.; Kihara, M.; Takayama, M.; Tanaka, H., Nondestructive Monitoring of Wood Decay Process Using FT-Raman Technique; Kami Parupu Kenkyu Happyokai Koen Yoshishu 2002, 69, 8–11.
30. Shen, Q.; Rahiala, H.; Rosenholm, J.B., Evaluation of the Structure and Acid–Base Properties of Bulk Wood by FT-Raman Spectroscopy; *J. Colloid Interface Sci.* 1998, 206, 558–568.
31. Yamauchi, S.; Shibutani, S.; Doi, S., Characteristic Raman Bands for Artocarpus Heterophyllus Heartwood; *J. Wood Sci.* 2003, 49, 466–468.
32. Edwards, H.G.M.; De Oliveira, L.F.C.; Nesbitt, M., Fourier-Transform Raman Characterization of Brazilwood Trees and Substitutes; *Analyst* 2003, 128, 82–87.
33. Holmgren, A.; Bergström, B.; Gref, R.; Ericsson, A., Detection of Pinosylvins in Solid Wood of Scots Pine Using Fourier Transform Raman and Infrared Spectroscopy; *J. Wood Chem. Technol.* 1999, 19, 139–150.
34. Nuopponen, M.; Willför, S.; Jääskeläinen, A.-S.; Sundberg, A.; Vuorinen, T.; A UV Resonance Raman (UVRR) Spectroscopic Study on the Extractable Compounds of Scots Pine (*Pinus sylvestris*) Wood. Part I: Lipophilic Compounds. *Spectrochim. Acta A* 2004, 60, 2953–2961.
35. Nuopponen, M.; Willför, S.; Jääskelainen, A.S.; Vuorinen, T., A UV Resonance Raman (UVRR) Spectroscopic Study on the Extractable Compounds in Scots Pine (*Pinus sylvestris*) Wood. Part II. Hydrophilic compounds; *Spectrochim. Acta A* 2004, 60, 2963–2968.

36. Wiley, J.H.; Atalla, R.H., Raman Spectra of Celluloses. In: Atalla, R.H. (ed.); *The Structures of Cellulose*, ACS Symposium Series 340; Washington, DC, 1987; pp. 151–168.
37. Halttunen, M.; Vyörykkä, J.; Hortling, B. *et al.*, Study of Residual Lignin in Pulp by UV Resonance Raman Spectroscopy; *Holzforschung* 2001, 55, 631–638.
38. Saariaho, A.-M.; Jääskeläinen, A.-S.; Nuopponen, M.; Vuorinen, T., Ultra Violet Resonance Raman Spectroscopy in Lignin Analysis: Determination of Characteristic Vibrations of *p*-Hydroxyphenyl, Guaiacyl and Syringyl Structures; *Appl. Spectrosc.* 2003, 57, 58–66.
39. Agarwal, U.P.; Atalla, R.H., Raman Spectral Features Associated with Chromophores in High-Yield Pulps; *J. Wood Chem.Technol.* 1994, 14, 227–241.
40. Agarwal, U.P.; Atalla, R.H., Using Raman Spectroscopy to Identify Chromophores in Lignin-Lignocellulosics. In: Glasser, W.G.; Northey, R.A.; Schultz, T.P. (eds); *Lignin: Historical, Biological, and Materials Perspectives*; ACS symposium series 742; American Chemical Society, Washington, DC, 2000; pp. 250–264.
41. Wiley, J.H.; Atalla, R.H., Band Assignments in the Raman Spectra of Celluloses; *Carbohydr. Res.* 1987, 160, 113–129.
42. Agarwal, U.P.; Ralph, S.A.; Atalla, R.H., FT Raman Spectroscopic Study of Softwood Lignin; Proc. 9th Intern. Symp. Wood Pulping Chem., *Canadian Pulp and Paper Assn.*; Montreal, 1997; pp. 8-1–8-4.
43. Agarwal, U.P.; McSweeny, J.D.; Ralph, S.A., An FT-Raman Study of Softwood, Hardwood, and Chemically Modified Black Spruce MWLs; Proc. 10th Intern. Symp. Wood Pulping Chem., Vol. II, Japan Technical Assn. Pulp & Paper Industry; TAPPI Press, Atlanta, GA, 1999; pp. 136–140.
44. Agarwal, U.P.; Weinstock, I.A.; Atalla, R.H., FT Raman Spectroscopy for Direct Measurement of Lignin Concentrations in Kraft Pulps; *Tappi J.* 2003, 2, 22–26.
45. Bujanovic, B.; Reiner, R.S.; Ralph, S.A.; Agarwal, U.P.; Atalla, R.H., Structural Changes of Residual Lignin of Softwood and Hardwood Kraft Pulp Upon Oxidative Treatment with Polyoxometallates; Proc. 2005 TAPPI Eng. Pulping Environ. Conf., Presentation Book 2, Paper # 30–3; TAPPI, Atlanta, GA, 2005.
46. Jääskeläinen, A.-S.; Saariaho, A.-M.; Vuorinen, T., Quantification of Lignin and Hexenuronic Acids in Bleached Hardwood Kraft Pulps: A New Calibration Method for UVRR Spectroscopy and Evaluation of the Conventional Methods; *J. Wood Chem. Technol.* 2005, 25, 51–65.
47. Saariaho, A.-M.; Jääskeläinen, A.-S.; Matousek, P.; Towrie, M.; Parker, A.W.; Vuorinen, T., Resonance Raman Spectroscopy of Highly Fluorescing Lignin Containing Chemical Pulps: Suppression of Fluorescence with an Optical Kerr Gate; *Holzforschung* 2004, 58, 82–90.
48. Agarwal, U.P.; Terashima, N., FT-Raman Study of Dehydrogenation Polymer (DHP) Lignins; Proc. 12th Intern. Symp. Wood Pulping Chem., Vol. III; Dept. of Forest Ecology and Management, University of Wisconsin, Madison, 2003; pp. 123–126.
49. Agarwal, U.P; Reiner, R.S.; Pandey, A.K.; Ralph, S.A.; Hirth, K.C.; Atalla, R.H., Raman Spectra of Lignin Model Compounds; Proc. 13th Inter. Symp. Wood Fiber Pulping Chem., Vol. 2; Appita, Carlton, Australia, 2005; pp. 377–384.
50. Agarwal, U.P.; Landucci, L.L., FT-Raman Investigation of Bleaching of Spruce Thermomechanical Pulp; *J. Pulp Paper Sci.* 2004, 30, 269–274.
51. Agarwal, U.P.; McSweeny, J.D., Photoyellowing of Thermomechanical Pulps: Looking beyond α-Carbonyl and Ethylenic Groups as the Initiating Structures; *J. Wood Chem. Technol.* 1997, 17, 1–26.
52. Ehrhardt, S.M., An Investigation of the Vibrational Spectra of Lignin Model Compounds, Ph.D. Thesis Dissertation, Institute of Paper Science and Technology, Atlanta, GA, 1984.
53. Larsen, K.L.; Barsberg, S.; Agarwal, U.P.; Elder, T., Prediction and Assignments of Vibrational Bands of Lignin Moieties by DFT; 231st American Chemical Society Meeting, Cell Division, March 26–31, ACS, Washington, DC, 2006, Abstract #7.

54. Saariaho, A.-M.; Argyropoulos, D.S.; Jääskeläinen, A.-S.; Vuorinen, T., Development of the Partial Least Squares Models for the Interpretation of the UV Resonance Raman Spectra of Lignin Model Compounds; *Vib. Spectrosc.* 2005, 37, 111–121.
55. Eichhorn, S.J.; Sirichaisit, J.; Young, R.J., Deformation Mechanisms in Cellulose Fibres, Paper and Wood; *J. Mater. Sci.* 2001, 36, 3129–3135.
56. Gierlinger, N.; Schwanninger, M.; Reinecke, A.; Burgert, I., Molecular Changes during Tensile Deformation of Single Wood Fibers Followed by Raman Microscopy; *Biomacromolecules* 2006, 7, 2077–2081.
57. Czaja, A.D.; Kudryavtsev, A.B.; Schopf, J.W., New Method for the Microscopic, Nondestructive Acquisition of Ultraviolet Resonance Raman Spectra from Plant Cell Walls; *Appl. Spectrosc.* 2006, 60, 352–355.
58. Vester, J.; Felby, C.; Nielsen, O.F.; Barsberg, S., Fourier Transform Raman Difference Spectroscopy for Detection of Lignin Oxidation Products in Thermomechanical Pulp; *Appl. Spectrosc.* 2004, 58, 404–409.
59. Barsberg, S.; Matousek, P.; Towrie, M., Structural Analysis of Lignin by Resonance Raman Spectroscopy; *Macromol. Biosci.* 2005, 5, 743–752.
60. Proniewicz, L.M.; Paluszkiewicz, C.; Weselucha-Birczynska, A.; Baranski, A.; Dutka, D., FT-IR and FT-Raman Study of Hydrothermally Degraded Groundwood Containing Paper; *J. Mol. Struct.* 2002, 614, 345–353.
61. Hunt, C.; Yu, X.; Bond, J.; Agarwal, U.; Atalla, R., Aging of Printing and Writing Papers upon Exposure to Light: Part 2-Mechanical and Chemical Properties; Proc. 12th Intern. Symp. Wood Pulping Chem., Vol. III; Dept. of Forest Ecology and Management, University of Wisconsin, Madison, 2003; pp. 231–234.
62. Jääskeläinen, A.-S.; Saariaho, A.-M.; Vyörykkä, J.; Vuorinen, T.; Matousek, P.; Parker, A.W., Application of UV-Vis and Resonance Raman Spectroscopy to Study Bleaching and Photoyellowing of Thermomechanical Pulps; *Holzforschung* 2006, 60, 231–238.
63. Agarwal, U.P.; Akhtar, M., Understanding Fungus-Induced Brightness Loss of Biomechanical Pulps; Proc. 2000 TAPPI Pulping, Process, and Product Quality Conference; TAPPI, Atlanta, GA, 2000; pp. 1–12.
64. Atalla, R.H.; Ranua, J.; Malcolm, E.W., Raman Spectroscopic Studies of the Structures of Cellulose: A Comparison of Kraft and Sulfite Pulps; *Tappi J.* 1984, 67, 96–99.
65. Saariaho, A.-M.; Hortling, B.; Jaaskelainen, A.-S.; Tamminen, T.; Vuorinen, T., Simultaneous Quantification of Residual Lignin and Hexenuronic Acid from Chemical Pulps with UV Resonance Raman Spectroscopy and Multivariate Calibration; *J. Pulp Paper Sci.* 2003, 29, 363–370.
66. Agarwal, U.P.; Reiner, R.S.; Ralph, S.A.; Using Nano- and Micro-Particles of Silver in Lignin Analysis; Proc. TAPPI Intern. Conf. Nanotechnol.; TAPPI Press, Atlanta, GA, April 26–28, 2006; NanoCD-06, ISBN 1-59510-121-7.
67. Potthas, A.; Rosenau, T.; Kosma, P.; Saariaho, A.-M.; Vuorinen T., On the Nature of Carbonyl Groups in Cellulosic Pulps; *Cellulose* 2005, 12, 43–50.
68. Niemelä, P.; Hietala, E.; Ollanketo, J.; Tornberg, J.; Pirttinen, E.; Stenius, P., FT-Raman Spectroscopy as a Tool for Analyzing the Composition of Recycled Paper Pulp; *Prog. Pap. Recycling* 1999, 4, 15–24.
69. Somwang, K.; Enomae, T.; Isogai, A.; Onabe, F., Changes in Crystallinity and Re-swelling Capability of Pulp Fibers by Recycling Treatment; *Japan Tappi J.* 2002, 56, 863–869.
70. Nuopponen M.; Vuorinen, T.; Jämsä, S.; Viitaniemi, P., Thermal Modifications in Softwood Studied by FT-IR and UV Resonance Raman Spectroscopies; *J. Wood Chem. Technol.* 2004, 24, 13–26.
71. Yamauchi, S.; Kurimoto, Y., Raman Spectroscopic Study on Pyrolyzed Wood and Bark of Japanese Cedar: Temperature Dependence of Raman Parameters; *J. Wood Sci.* 2003, 49, 235–240.

72. Yamauchi, S.; Iijima, Y.; Doi, S., Spectrochemical Characterization by FT-Raman Spectroscopy at Low Temperatures: Japanese Larch and Beech; *J. Wood Sci.* 2005, 51, 498–506.
73. Kurti, E.; Heyd, D.V.; Wylie, R.S., Raman Microscopy for the Quantitation of Propiconazole in White Spruce; *Wood Sci. Technol.* 2005, 39, 618–629.
74. Gierlinger, N.; Hansmann, C.; Röder, T.; Sixta, H.; Gindl, W.; Wimmer, R., Comparison of UV and Confocal Raman Microscopy to Measure the Melamine–Formaldehyde Resin Content Within Cell Walls of Impregnated Spruce Wood; *Holzforschung* 2005, 59, 210–213.
75. Scheepers, M.L.; Gelan, J.M.; Carleer, R.A. *et al.*, Investigation of Melamine–Formaldehyde Cure by Fourier Transform Raman Spectroscopy; *Vib. Spectrosc.* 1993, 6, 55–69.
76. Yamauchi, S.; Tamura, Y.; Kurimoto, Y.; Koizumi, A., Vibrational Spectroscopic Studies on Wood and Wood Based Materials. III. Identification of Adhesives in Wood by Using FT-Raman Spectroscopy as a Nondestructive Analytical Method; *Nippon Setchaku Gakkaishi* 1997, 33, 380–388.
77. Yamauchi, S.; Doi, S., Raman Spectroscopic Study on the Behavior of Boric Acid in Wood; *J. Wood Sci.* 2003, 49, 227–234.
78. Agarwal, U.P.; Reiner, R.S.; Ralph, S.A., Dependable Cellulose I Crystallinity Determination using Near-IR FT-Raman; CELL Division, Abstract 95, 233rd ACS National Meeting; Chicago, March 25–29, 2007.
79. Agarwal, U.P.; Kawai, N., Self-Absorption Phenomenon in Near-Infrared Fourier Transform Raman Spectroscopy of Cellulosic and Lignocellulosic Materials; *Appl. Spectrosc.* 2005, 59, 385–388.

In: Characterization of Lignocellulose Materials, Chapter 2, edited by Thomas Q. Hu, Blackwell Publishing, Oxford, UK; pp. 17-35; 2008